Malaysian Journal of Analytical Sciences (MJAS)
Published by Malaysian Analytical Sciences Society

# RECOVERED PALLADIUM COMPLEXES AS A POTENTIAL HOMOGENEOUS CATALYST FOR C-H FUNCTIONALIZATION AND ANTIBACTERIAL AGENT

## (Kompleks Palladium Dipulihkan sebagai Pemangkin Homogen untuk Fungsi C-H dan Ejen Antibakteria)

Nur Anis Nabilah Mohd Fuzi[1], Siti Khadijah Rahmat[1], Muhammad Hazim Abdul Aziz[1], Mohammad Noor Jalil[1], Shamsul Bahrin Gulam Ali[2*], and Khairil Anuar Jantan[1*]

[1]*School of Chemistry and Environment,*
*Faculty of Applied Sciences*
*Universiti Teknologi MARA,*
*40450 Shah Alam, Selangor, Malaysia*
[2]*Faculty of Health Sciences, Bertam Campus*
*Universiti Teknologi MARA,*
*13200 Kepala Batas, Penang, Malaysia*

[*]*Corresponding author: sbahrin@uitm.edu.my & khairil0323@uitm.edu.my*

Received: 24 August 2022; Accepted: 9 December 2022; Published: 19 April 2023

**Abstract**

The present study describes the utilization of simple and commercially available iodine and tetraphenylphosphonium salt as leaching agents to recover palladium (Pd) from waste. This study employed a model reaction assay that utilized Pd(0) metal powder to stimulate palladium leaching from spent automotive three-way catalyst (TWC). The palladium complexes, $(Ph_4P)_2[Pd_2I_6]$, obtained were characterized with Fourier-transform infrared (FT-IR), ultraviolet-visible (UV-Vis) spectroscopy, nuclear magnetic resonances (NMR), thermogravimetric analysis (TGA), and elemental analysis. The recovered Pd complexes demonstrated excellent catalytic activity towards the methoxylation of benzo[*h*]quinoline. Furthermore, a lower to moderate product yield was recorded for the ethoxy- and isopropoxylation of benzo[*h*]quinoline. The C-H functionalization of 8-methylquinoline catalyzed by the obtained palladium complexes also documented a moderate product yield (< 65%) after 6 hours of reaction. The antibacterial activities of the $(Ph_4P)_2[Pd_2I_6]$ were evaluated through a disk diffusion test, minimum inhibitory concentration (MIC), and minimum bactericidal concentration (MBC) assays. Among the gram-positive and -negative bacteria evaluated, *Klebsiella pneumoniae* exhibited the highest sensitivity to the synthesized $(Ph_4P)_2[Pd_2I_6]$ at all concentrations. The MIC concentrations for all assessed bacteria ranged from 0.156 to 1.25 mg/mL. Moreover, bacterial growth was detected in all MBC plates, thus indicating that the $(Ph_4P)_2[Pd_2I_6]$ possessed a bacteriostatic effect and not a killing attribute.

**Keywords:** recovered palladium, palladium catalyst, antibacterial activity

**Abstrak**

Kajian ini menghuraikan mengenai penggunaan iodin dan garam tetrafenilphosphonium yang mudah dan boleh didapati secara

komersial sebagai agen larut lesap dalam proses pemulihan paladium (Pd) daripada sisa terbuang. Kajian ini melaksanakan ujian berdasarkan model tindak balas yang menggunakan serbuk logam Pd(0) untuk merangsang proses larut lesap Pd dari pemangkin tiga hala automotif (TWC) terpakai. Spesies molekul kompleks Pd dipulihkan, $(Ph_4P)_2[Pd_2I_6]$, yang diperoleh dicirikan melalui Fourier-transform inframerah (FT-IR), spektroskopi ultra ungu-nampak (UV-Vis), resonans magnet nuklear (NMR), analisis termogravimetrik (TGA) dan analisis unsur. Kompleks Pd dipulihkan yang diperoleh tersebut menunjukkan aktiviti pemangkin yang sangat baik bagi ke arah metoksilasi benzo[*h*]kuinolin. Selain itu, hasil produk yang sederhana telah direkodkan bagi etoksi dan isopropoksilasi benzo[*h*]kuinolin. Kefungsian C-H sebagai pemangkinan 8-metilquinolin oleh kompleks Pd dipulihkan juga merekodkan hasil produk yang sederhana (< 65%) selepas tindak balas selama 6 jam. Aktiviti antibakteria $(Ph_4P)_2[Pd_2I_6]$ tersebut dinilai melalui ujian resapan cakera, kepekatan perencatan minimum (MIC), dan ujian kepekatan bakteria minimum (MBC). Antara kesemua bakteria gram-positif dan -negatif yang diuji, *Klebsiella pneumoniae* menunjukkan sensitiviti tertinggi kepada $(Ph_4P)_2[Pd_2I_6]$ pada semua kepekatan. Kepekatan MIC untuk semua bakteria yang diuji direkod dalam julat 0.156 hingga 1.25 mg/ml. Tambahan pula, pertumbuhan bakteria yang dikesan dalam semua plat MBC menunjukkan bahawa $(Ph_4P)_2[Pd_2I_6]$ mempunyai kesan bakteriostatik dan tidak membunuh.

**Kata kunci:** paladium dipulihkan, mangkin paladium, aktiviti antibakteria

## Introduction

Palladium (Pd) is a limited and significant raw material due to its scarcity and economic value [1]. Consequently, the element possesses a considerable market demand, dominated by automotive catalytic converters and electronic equipment, which account for 90% of its global production [2]. Nonetheless, Pd is primarily mined in geopolitically-unstable countries, such as Russia and South Africa, which could affect supply and pricing [3]. Furthermore, Pd mining is an energy-intensive process that employs chemical reagents [4] that are exceptionally detrimental to the environment, including published harmful effects on water and air quality, biodiversity, and housing displacement [5-7]. Consequently, a practical and realistic approach is necessary for sustainable Pd utilization.

The Pd-containing waste from three-way catalytic converters (TWC) [8] and electric and electronic equipment (EEE) [9] has accumulated worldwide. The substance is a significant but underutilized source of potentially recoverable raw material. The most common techniques for recovering Pd from waste include pyro- and hydrometallurgical methods, where both are disadvantageous. The pyrometallurgical method consumes high energy and lacks Pd selectivity [10]. The more selective hydrometallurgical techniques rely on harmful reagents, such as potent oxidizing agents, including aqua regia and cyanide to leach Pd from spent TWC and EEE under mild conditions [11].

Available energy-efficient and sustainable recovery techniques produce molecular recovery products. Serpe and colleagues [12] demonstrated an excellent method of utilizing organic compounds, such as N,N'-dimethylperhydrodiazepine-2,3-dithione diiodine adduct ($Me_2dazdt{\cdot}2I_2$), to recover Pd from model spent catalytic converter under mild conditions. Nevertheless, the recovered Pd complexes $[Pd(Me_2dazdt)_2]I_6$ require an energy-intensive step that eliminates its ligands to procure metallic Pd as the end product [12].

An intriguing application was proposed by Wilton-Ely *et al*. to utilize the recovered Pd complex directly as a homogeneous catalyst in the C-H functionalization of benzo[*h*]quinoline and 8-methylquinoline [13]. Surprisingly, the $[Pd(Me_2dazdt)_2]^{2+}$ was catalytically active toward the proposed reaction, thus outperforming the conventionally mined $Pd(OAc)_2$ [14]. Nonetheless, the relatively expensive starting materials and Lawesson's reagent employed to install sulfur groups into the ligand designs diminished the economic and environmental benefits of the recovery process. Accordingly, a simpler, cheaper, and commercially available approach was sought to address the constraint. The impressive ability of organic triiodides, tetraphenylphosphonium $[Ph_4P]^+$, in the presence of iodine in the selective dissolution of Pd from spent TWCs was demonstrated by [15] (see Scheme 1).

The present study directly utilized the recovered Pd complexes, $(Ph_4P)_2[Pd_2I_6]$, as a homogeneous catalyst in the C-H functionalization of benzo[*h*]quinoline and

8-methylquinoline in ambient air, which required nitrogen as the only directing atom. The procedures were based on the work by [13]. The Pd loading, temperature, and time were varied to optimize the catalytic reaction. The lower temperature approach was focused on enhancing the green credential of the method. The results were compared to previous findings in studies utilizing different Pd catalysts obtained from commercial or secondary sources.

The recent emergence of antimicrobial resistance has become a critical issue worldwide [16]. Consequently, the demand to develop novel and efficient antimicrobial agents has also increased. Numerous studies have attempted to elucidate Pd compound potentials in combating human pathogens-caused illnesses [17–21]. Nonetheless, only very few studies reported the possible effects of recovered Pd against pathogenic bacteria. Thus, the present study explored the antibacterial attributes of the recovered $(Ph_4P)_2[Pd_2I_6]$ against common gram-positive and -negative bacteria.

## Materials and Methods

All chemicals and solvents employed in the present study were purchased and utilized without further purification unless otherwise stated.

### Synthesizing the $(Ph_4P)_2[Pd_2I_6]$ complexes

Serpe and co-workers [15] demonstrated the impressive ability of tetraphenylphosphonium $[Ph_4P]^+$ in the selective dissolution of Pd from spent TWCs (see Scheme 1). The Pd metal powder was employed as a proxy for the milled TWC mixed-metal powder to assess the Pd complex generated by the system. Tetraphenylphosphonium iodide (0.144 g, 0.31 mmol) was treated with iodine in acetone (30 mL) before adding Pd metal powder (33.1 mg, 0.31 mmol). The reaction mixture was stirred at room temperature for 3 hours until an abundant black crystalline product was precipitated. Subsequently, product re-crystallization was conducted by slowly diffusing diethyl ether into the concentrated acetone solution of the reaction mixture. The yield recorded in this study was 286 g (90%) [15].

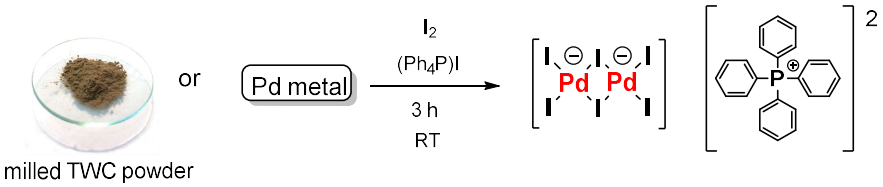


Scheme 1. The synthesis of recovered Pd complexes [15]

### Characterization of $(Ph_4P)_2[Pd_2I_6]$ complexes

The Pd complexes obtained in the current study were characterized via $^1H$ and $^{13}C$ nuclear magnetic resonance (NMR) with a JEOL JNM-ECZS 400 MHz spectrometer. A Varian Bruker AV300 spectrometer was also employed in attributing the $^1H$ NMR signals of the C-H functionalization catalysis reaction at 25 °C with deuterated chloroform ($CDCl_3$). Moreover, infra-red data were obtained with a Nicolet 6700 ATR spectrometer at 16 scans of 600–4000 $cm^{-1}$ on solid samples. The specimens were also subjected to an ultraviolet-visible (UV-VIS) spectrometer (Perkin Elmer Lambda 25) to obtain the transmission and absorption spectra of the complexes within the 300–800 nm wavelength. Furthermore, elemental analyses (EA) were performed with CHNS/O Analyzer 2400 Perkin Elmer Series II, while thermogravimetric analysis (TGA) was conducted in a nitrogen atmosphere with a Mettler Toledo TGA/DSC 1LF/UMX.

### The general C-H functionalization synthetic procedure

The C-H functionalization reaction in this study was performed with a Radley's Carousel 12 Reaction Station. The adaptable apparatus transforms a normal stirring hotplate into 12 parallel synthesizers capable of conducting parallel chemical reactions in an inert or ambient environment. First, individual reaction bottles (24 mm × 150 mm) were filled with alcohols, sacrificial oxidants, Pd catalysts, and substrates. The reaction

bottles were then installed on the Carousel 12 Reaction Station before the mixture was heated and stirred for 2, 4, and 6 hours. The operational temperature range of the heated base was 0–180°C at ±0.5 °C temperature precision. A single spinning magnetic field was also applied to ensure homogeneous stirring in each reaction bottle.

Figure 1. Radley's Carousel 12 Reaction Station

**Synthesizing 10-alkoxybenzo[*h*]quinoline**

Benzo[*h*]quinoline (50.0 mg, 0.28 mmol), (diacetoxyiodo)benzene (180.4 mg, 0.56 mmol), and $(Ph_4P)_2[Pd_2I_6]$ (between 1–2 mol% loads) were mixed in 2.5 mL alcohol [methanol (MeOH), ethanol (EtOH), or isopropanol and glacial acetic acid mixture] in a reaction bottle. Subsequently, individual reaction bottles were heated at 50 and 100 °C and stirred for 2, 4, and 6 hours. All solvent was then removed with a rotary evaporator, followed by the dissolution of the residue in a deuterated $CDCl_3$ for $^1$H NMR analysis (see Scheme 2).

The $^1$H NMR spectroscopic yield analysis was conducted by comparing the integration of the $H_2$ or $H_{10}$ protons of benzo[*h*]quinoline at 9.30 and 9.05 ppm, respectively, to the peak of 10-alkoxybenzo[*h*]quinoline at 9.15 ppm. Another peak corresponding to the alkoxy group in the product was subjected to further evaluation at 4.19 (methoxy, $CH_3$; singlet), 1.63 and 4.45 (ethoxy, $CH_2CH_3$; triplet and quartet), and 1.54 and 4.76 [isopropoxy, $CH(CH_3)_2$; doublet and septet] ppm. All reactions were conducted a minimum of three times, and the yields were measured with $^1$H NMR based on three independent experiments.

Benzo[*h*]quinoline (150.0 mg, 0.84 mmol), (diacetoxyiodo)benzene (541.2 mg, 1.68 mmol), and $(Ph_4P)_2[Pd_2I_6]$ (2 mol%) were treated in MeOH (7.5 mL) and heated at 50 °C for 2 hours for the isolated yield reaction. The products were then purified in a flash column (3:2 v/v ethyl acetate-to-n-hexane eluent) to procure 10-methoxybenzo[*h*]quinoline.

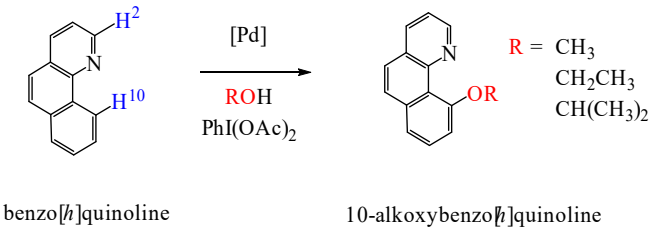


Scheme 2. The benchmark reaction for oxidative C-H functionalization

**The synthesis of 8-(methoxymethyl)quinoline**

A total of 42.5 mg of 8-methylquinoline (0.297 mmol), 103.3 mg of (diacetoxyiodo)benzene (0.321 mmol), and between 1–2 mol% loadings of $(Ph_4P)_2[Pd_2I_6)$ were mixed in 2.5 mL MeOH in reaction bottles. The individual reaction bottles were then heated at 50 °C and stirred for 2, 4, and 6 hours. Subsequently, the solvent was removed under reduced pressure, followed by the dissolution of the residue obtained in a deuterated $CDCl_3$ for $^1$H NMR analysis. The product yield was determined by comparing the methyl integration (2.82 ppm) of 8-methylquinoline with the methylene (5.19 ppm) and methoxy group (3.57 ppm) in the 8-(methoxymethyl)quinoline resonances (see Scheme 3).

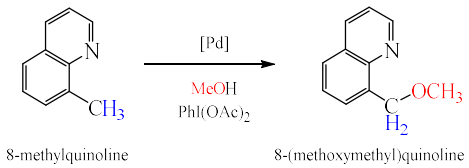


Scheme 3. The C-H functionalization of 8-methyl quinolone

**Bacterial culture**

Stock cultures of gram-negative, *Escherichia coli* (ATCC25922), *Salmonella typhimurium* (ATCC14028), *Klebsiella pneumoniae* (ATCC700603), and *Klebsiella aeruginosa* (ATCC13048), and gram-positive bacteria, *Bacillus cereus* (ATCC11778) and *Bacillus subtilis* (ATCC13124), were obtained from the Faculty of Applied Sciences, Universiti Teknologi MARA (UiTM), Shah Alam. The cultures were maintained on nutrient agar media at 37 ℃. Colony morphology observation and gram staining were performed in the present study to confirm the working strains.

**Antimicrobial study: Disk diffusion method**

The antibacterial activities of varying concentrations of $(Ph_4P)_2[Pd_2I_6]$ complex were screened against common gram-positive and -negative bacteria. Subsequently, the antibacterial activities of the samples were determined with the Kirby-Bauer disk diffusion method on a Muller-Hinton Agar (MHA) medium. For working cultures, 18–20 hours broth culture of each bacterium inoculum was compared with 0.5 McFarland standard ($1 \times 10^8$ CFU/mL) and adjusted visually to obtain working cultures. A sterile cotton swab was dipped into the McFarland standardized inoculum, seeded and covered the MHA plate with the evenly swabbed inoculum. Next, sterile disks were placed onto each plate.

Before analysis, the $(Ph_4P)_2[Pd_2I_6]$ was dissolved in dichloromethane (DCM) into varying concentrations (1, 2, 3 and 4 mg/mL). An amount of 20 $\mu$L of each $(Ph_4P)_2[Pd_2I_6)$ concentration was pipetted onto the disks. Gentamicin (CN) (10 µg) and sterile distilled water were utilized as positive and negative controls, respectively. All of the plates were then incubated for 24 hours at 37 ℃. Following incubation, the inhibitory zone (in mm) was measured and recorded. All tests were performed in triplicate per condition.

**The MIC and MBC**

MIC was determined using Mueller–Hinton broth (MHB) macrodilution assays. Briefly, bacteria inoculum was prepared and adjusted to McFarland standard as before. Next, 1 mL of adjusted inoculum was transferred into 8 sterile test tubes. 1 mL of $(Ph_4P)_2[Pd_2I_6]$ complex dissolved in DCM was then added into the first tube, and 2-fold serial dilutions were performed to give the final concentrations of 10, 5, 2.5, 1.25, 0.625, 0.313, 0.156 and 0.078 mg/mL. Two additional tubes were prepared as positive growth control (MHB + bacteria) and negative control (MHB only). All tubes (in triplicate per condition) were incubated aerobically for 24 hours at 37 ℃, and MIC values were determined as the lowest concentration of the test compound that prevents microbial growth. For MBC, the MIC tubes that showed no visible apparent growth were subcultured onto the MHA plate and incubated for 24 hours at 37 ℃. No evidence of bacterial growth following incubation were confirmed as MBC values.

**Statistical analysis**

For antimicrobial analysis, data were statistically analyzed using GraphPrism 8.0. Results for the inhibitory zone were expressed as means ± standard error of the means (SEM). The results shown are the mean of three tested cultures plus SEM. Data were further analyzed with a two-way Analysis of Variance (ANOVA) followed by a Tukey's multiple comparison post-test. In all tests, p-values <0.05 and asterisks indicate statistically significant differences.

## Results and Discussion

**Transformation of recovered Pd complex from the recovery process**

Scheme 1 illustrates selective Pd leaching from waste utilizing an organic triiodide salt in an organic solution

at room temperature. The peculiar features of the iodide/iodine mixture in the tetraphenylphosphonium iodide [($PPh_4$)I] system could dissolve and quantitatively recover Pd from spent automotive TWC waste, generating a molecular $(Ph_4P)_2[Pd_2I_6]$ species [15]. Nonetheless, the procedure necessitates conventional thermal treatment to procure metallic Pd as the end product, thus making the technique less practical for recycling Pd. Consequently, the $(Ph_4P)_2[Pd_2I_6]$ complex obtained directly as a homogeneous catalyst for C-H activation and antibacterial agent against common pathogenic bacteria was suggested to solve the issue.

This study employed Pd metal powder as a proxy for milled TWC metal powder mix to generate the recovered Pd complex $(Ph_4P)_2[Pd_2I_6]$. Equimolar Pd powder with ($PPh_4$)I and iodine was dissolved in an acetone solution. The reaction mixture was stirred at room temperature for 3 hours. The resultant abundant black crystals formed were collected. The products were then re-crystallized by slowly diffusing diethyl ether ($Et_2O$) in a concentrated $(Ph_4P)_2[Pd_2I_6]$ acetone solution. A good yield of 90% was recorded. The infra-red and UV-Vis analysis of the $(Ph_4P)_2[Pd_2I_6]$ obtained in this study agreed well with the data reported by [15]. The complex was further characterized with NMR spectroscopy and elemental analysis to confirm the overall molecular formula.

**The FT-IR analysis of the $(Ph_4P)_2[Pd_2I_6]$ chemical composition**

The vibration frequencies of the $[PPh_4]^+$ counter ions remained virtually unchanged upon the Pd complex formation (see Figure 2). Furthermore, typical C-H and C-P stretching in aromatic phenyl absorptions were observed at 3049 and 1105 $cm^{-1}$, respectively. The aromatic C-H in-plane bending was also observed around the 1433 $cm^{-1}$ region. The C-H bending for the monosubstituted absorption band was obscured within the 751–682 $cm^{-1}$ band. The C=C and C-C stretching feature retentions in the infrared spectrum were observed at 1584 and 1479–1433 $cm^{-1}$, respectively [22]. The Pd-I stretching frequencies were not detected due to the absorption band occurring at a lower frequency region, while the other stretches agreed with a previous report [15].

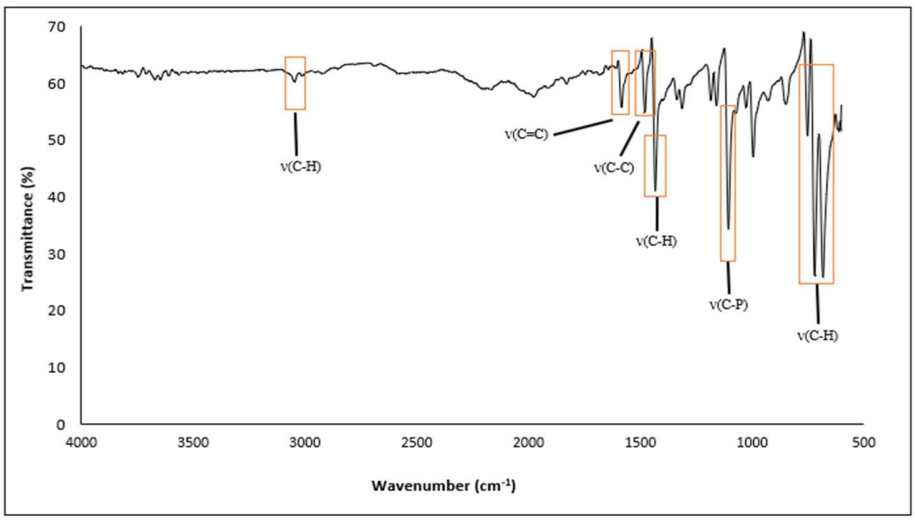


Figure 2. The FT-IR spectra of the recovered $(Ph_4P)_2[Pd_2I_6]$ complex

**The $(Ph_4P)_2[Pd_2I_6]$ complexation analysis with UV-Vis spectra**

Figure 3 illustrates the UV-Vis spectra of the Pd complexes procured in the current study. The presence of dimeric Pd complex, $[Pd_2I_6]^{2-}$, was confirmed by the absorption at 340 nm, while the peaks recorded at 426 and 524 nm supported the report by [15]. The absorption of $PPh_4^+$ was documented at approximately 260 nm, but

absorptions below 300 nm were indistinct and could not be appropriately determined [23].

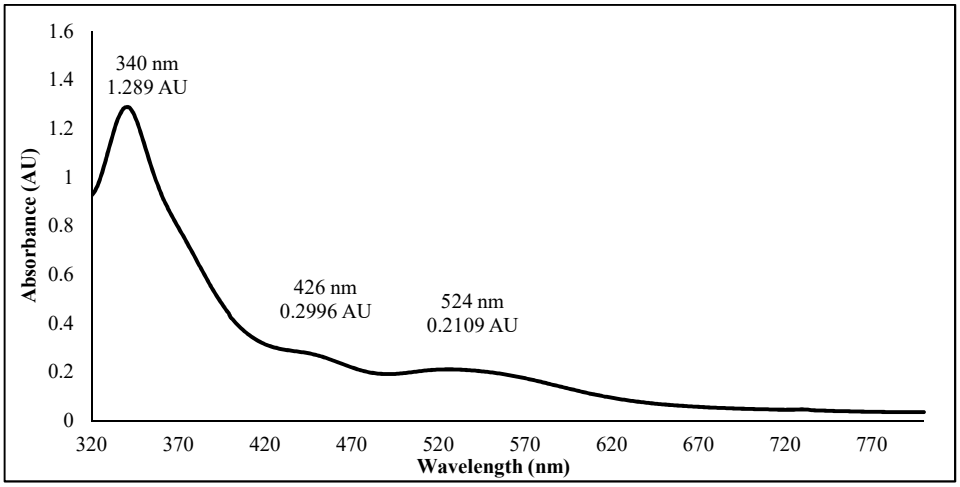


Figure 3. The UV-Vis spectra of the recovered $(Ph_4P)_2[Pd_2I_6]$ complex

**The $(Ph_4P)_2[Pd_2I_6]$ molecular structure analysis via NMR spectroscopy**

The NMR spectra of the $(Ph_4P)_2[Pd_2I_6]$ complex procured in this study were recorded in deuterated $CDCl_3$. The $^1H$ NMR analysis revealed diagnostic features of multiplet resonances at aromatic regions (7.66–7.95 ppm), which were attributed to the aromatic protons of the $[PPh_4]^+$ counter-ion phenyl groups. The carbon nuclei of $[PPh_4]^+$ counter-ions were almost unaltered compared to the precursors in the $^{13}C$ NMR spectrum. The $^1H$ NMR was set to 400 MHz, δ 7.95–7.66 ppm, while the $^{13}C$ NMR was at δ 117.0, 117.1, 131.0, 131.2, 134.7, 134.8, and 135.8 ppm.

**The $(Ph_4P)_2[Pd_2I_6]$ organic matter composition analysis with CHNS/O analyzer**

The composition of organic matter in the Pd complex $[C_{48}H_{40}I_6P_2Pd_2$ (Mw = 1653.06 g/mol)] obtained in the present study was determined with a CHNS/O analyzer. The results revealed experimental and calculated carbon and hydrogen percentages agreement, thus confirming the organic matter composition in the complex (see Table 1).

Table 1. Elemental analysis of the $(Ph_4P)_2[Pd_2I_6]$ complex

| Element | Atomic Weight (g/mol) | Calculated Weight (%) | Experimental Weight (%) |
|---|---|---|---|
| C | 12.011 | $\frac{12.011 \times 48 \times 100}{1653.06} = 34.87$ | 34.9 |
| H | 1.008 | $\frac{1.008 \times 40 \times 100}{1653.06} = 2.44$ | 2.4 |

**Thermal stability analysis of the $(Ph_4P)_2[Pd_2I_6]$ with TGA**

The thermal stability of the $(Ph_4P)_2[Pd_2I_6]$ complex from 30 to 750 °C was assessed at a 10 °C per minute heating rate (see Figure 4). The TGA isotherm exhibited slow mass declines within 30–300 °C before decreasing

significantly from 300 to 380 °C, indicating a 63% weight loss during the first stage of decomposition. The second stage of thermal decomposition was documented within 380–460 °C with a weight loss of approximately 17%. The loss in mass was relatively stable throughout the analysis. The stability of the complexes at high temperatures allowed the catalytic C-H functionalization reaction to be conducted at 100 °C.

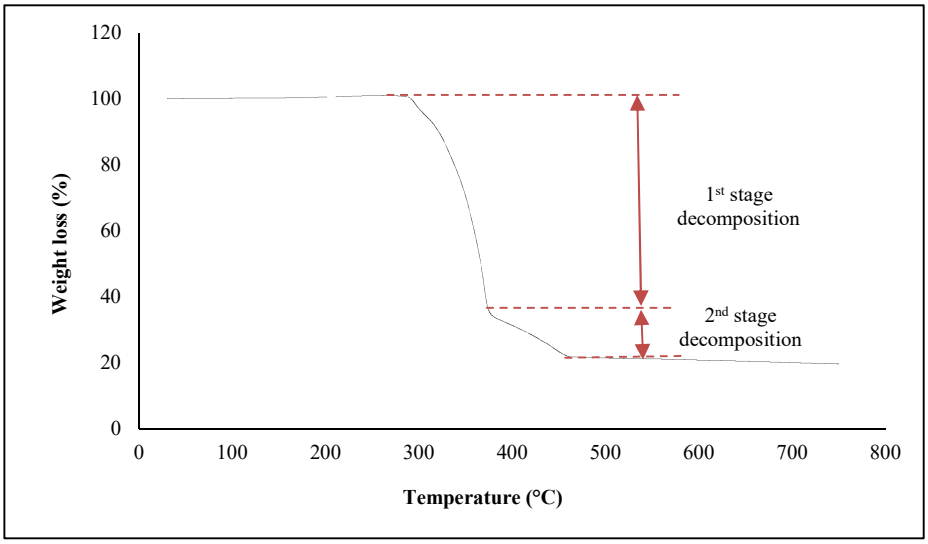


Figure 4. The TGA isotherm of the $(Ph_4P)_2[Pd_2I_6]$ complex

**The catalytic activity of the $(Ph_4P)_2[Pd_2I_6]$ complex towards methoxylation of benzo[*h*]quinoline**

The first comprehensive studies of Pd (II) complexes catalyzed C-H functionalization were published in the 2000s. A successful methoxylation of benzo[*h*]quinoline (see Scheme 2) in the presence of Pd acetate (1.1 mol%), the catalyst, and (diacetoxyiodo)benzene, the sacrificial oxidant, in MeOH was reported by Dick et al. [14]. Suitable high-pressure vials heated in an aluminium heating block to 100 °C were utilized in the study to yield a 95% product after 22 hours (see Table 2). In a similar manner, an 87% yield of 10-methoxybenzo[*h*]quinoline by employing recovered Pd complex, $[Pd(Me_2dazdt)_2]I_6$, (1 mol%) in 2 hours reaction time at 100°C was documented by Jantan et al. [13].

The present study slightly modified the procedure and utilized a Radley's Carousel 12 Reaction Station to investigate the catalytic activity of the recovered $(Ph_4P)_2[Pd_2I_6]$ complex towards methoxylation of benzo[*h*]quinoline (1 mol%, 2 hours, 100 °C). A quantitative product yield (90%) was obtained in 2 hours, which indicated that the reaction was more facile than the conditions documented in previous literature. The findings emphasized that the catalytic mechanism involved an oxidative addition step occured and resulted in the cyclopalladation of Pd (II) and oxidized Pd(II) to Pd(IV) before being followed by reductive elimination [14].

Table 2. Summary of catalytic activity various catalysts toward methoxylation of benzo[*h*]quinoline

| Solvent | Temperature (°C) | Catalyst | Catalyst Loading (mol%) | Time (h) | NMR yield (%) |
|---|---|---|---|---|---|
| MeOH | 100 | $Pd(OAc)_2$ | 1.1 | 22 | 95 |
| | | $[Pd(Me_2dazdt)_2]I_6$ | 1.0 | 2 | 87 |
| | | $(Ph_4P)_2[Pd_2I_6]$ | 1.0 | 2 | 90 |

Heating MeOH (b.p. 65 °C) at 100 °C in a confined space, such as vials, could lead to potential dangers related to build-up pressure. Furthermore, energy consumption reduction from high-temperature heating is preferable. Consequently, the study decreased the reaction temperature (T) to 50 °C without changing other parameters to lower the catalytic reaction energy usage. Resultantly, a higher product yield (89%) was obtained in 2 hours of reaction time with the $(Ph_4P)_2[Pd_2I_6]$ (1 mol%) employed as a catalyst (see Figure 5). Elevating the reaction time to 6 hours also resulted in a slightly enhanced product percentage procurement (93%–96%). Moreover, an increased Pd loading by one-fold recorded a quantitative product yield of > 90%. Overall, the approach employed in this study involved milder and safer conditions and shorter reaction times.

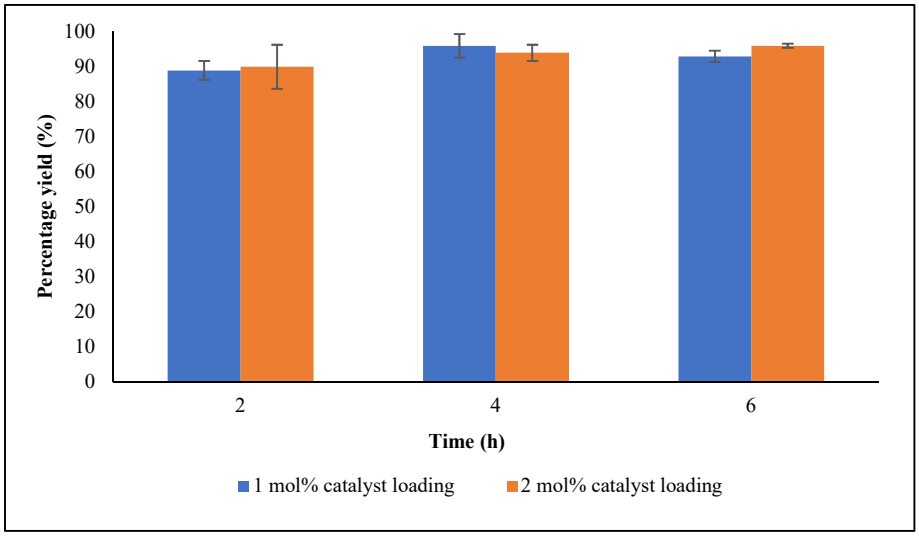


Figure 5. Methoxylation of benzo[*h*]quinoline with the $(Ph_4P)_2[Pd_2I_6]$ complex as a catalyst. Note: Solvent = MeOH, oxidant = $PhI(OAc)_2$, T = 50 °C, and t = 2, 4, and 6 hours

The successful formation of the product was further confirmed by analyzing the isolated yields of methoxylation of benzo[*h*]quinoline. The assessment was set to 2 hours of reaction time and 2 mol% of catalyst loading at 50 °C. The evaluation also validated the $^1$H NMR integration yield. A brown oil was collected and purified in a flash column utilizing a 3:2 v/v ethyl acetate-to-hexane eluent. The pale-yellow solid isolated (154 mg, 88%) also agreed with the conversion determined in the $^1$H NMR (90%).

**Other alkoxylation of benzo[*h*]quinoline**

The unexpectedly higher 10-methoxybenzo[*h*]quinoline procured at 50 °C resulted in the extension of the scope of this study into other alkoxylation of benzo[*h*]quinoline (see Scheme 2). In the assessment, the time and Pd loading were varied while the temperature was maintained at 50 °C. Furthermore, the alcohol solvent employed in the transformation was changed to ethanol and an isopropanol and acetic acid mixture, which yielded 10-ethoxybenzo[*h*]quinoline and 10-isopropoxybenzo[*h*]quinoline, respectively.

Figure 6 illustrates the experimental data of ethoxylation of benzo[*h*]quinoline at 50 °C. The 1 mol% catalyst loading produced a lower product yield (< 40%) even after 6 hours of reaction, hence implying that a temperature decrease reduces the chemical reaction rate. Nonetheless, elevating the catalyst loading to 2 mol% improved the reaction rate, which resulted in 79% yields of the desired products after 6 hours of reaction.

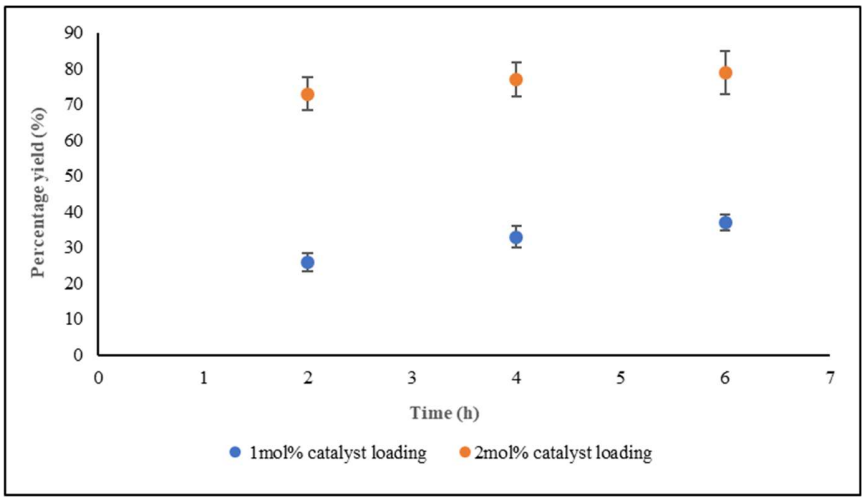


Figure 6. Ethoxylation of benzo[*h*]quinoline with the $(Ph_4P)_2[Pd_2I_6]$ complex as a catalyst. Note: Solvent = EtOH, oxidant = $PhI(OAc)_2$, T = 50 °C, and t = 2, 4, and 6 hours

A similar observation was recorded in the catalytic 10-isopropoxy benzo[*h*]quinoline reaction. Figure 7 indicates that a lower product yield (< 27%) was obtained when 1 mol% of catalyst loading was employed for reaction times between 2-6 hours at 50 °C. The results suggested that only a small proportion of benzo[*h*]quinoline molecules possess enough activation energy to react and generate a 10-isopropoxy benzo[*h*]quinoline at lower temperatures.

The increment of the catalyst loading to 2 mol% improved the reaction, which doubled the product yield. Nevertheless, a moderate 10-isopropoxybenzo[*h*]quinoline production (47%) was obtained compared to the 10-ethoxybenzo[*h*]quinoline (79%) derived after 6 hours when 2 mol% catalyst loading was employed at 50 °C. The results proved that the $(Ph_4P)_2[Pd_2I_6]$ was less catalytically active when the more sterically demanding reagent, the isopropanol and acetic acid mixture, was employed.

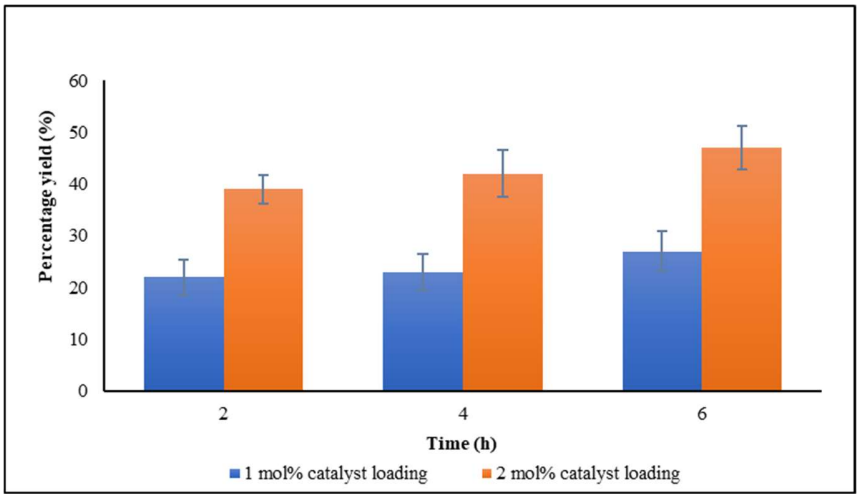


Figure 7. Isopropoxylation of benzo[*h*]quinoline utilizing the $(Ph_4P)_2[Pd_2I_6]$ complex as a catalyst. Note: Solvent = mixture of isopropanol and acetic acid, oxidant = $PhI(OAc)_2$, T = 50 °C, and t = 2, 4, and 6 hours

**The C-H functionalization of 8-methylquinoline**

The present study extended the catalytic alkoxylation of benzo[*h*]quinoline to synthesize 8-(methoxymethyl)quinoline (see Scheme 3). An energy-saving strategy by reducing the reaction temperature was adopted during the present study to continue building greener synthetic pathways and improve the efficiency of the required C-H functionalization. Nevertheless, the reaction of 8-methylquinoline with 1–2 mol% of the recovered $(Ph_4P)_2[Pd_2I_6]$ as the catalyst and $PhI(OAc)_2$ in methanol at 50 °C recorded a moderate yield (< 65%) after 2–6 hours of reaction time (see Figure 8). A possible explanation might be the presence of additional benzylic hydrogen atoms in the substrate, which are inert to deprotonation for directed C-H activation. Consequently, increasing the catalyst load or temperature while maintaining other reaction conditions might be required to lower the activation energy of the reaction for complete conversion.

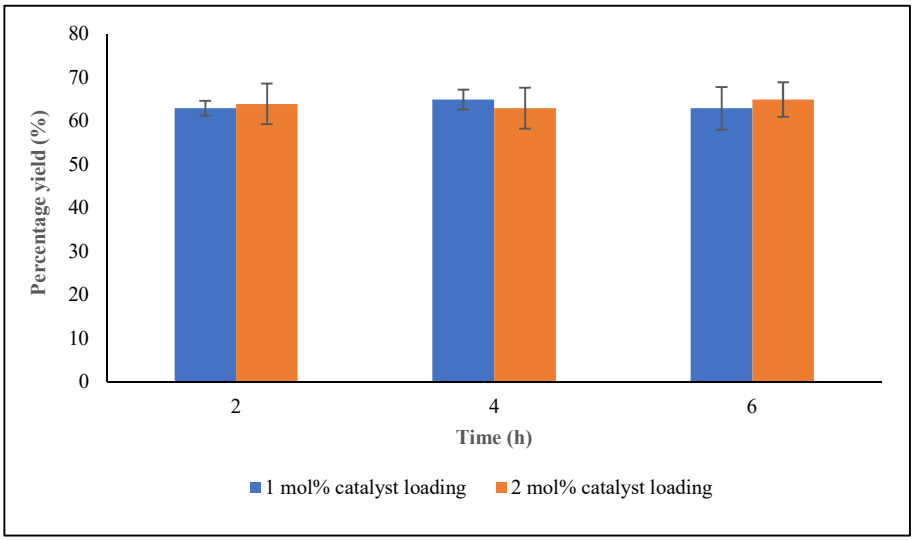


Figure 8. The C-H functionalization of 8-methylquinoline with the $(Ph_4P)_2[Pd_2I_6]$ complex as a catalyst. Note: Solvent = MeOH, oxidant = $PhI(OAc)_2$, T = 50 °C, and t = 2, 4, and 6 hours

**Antibacterial activity**

The antibacterial inhibition zone diameter means of the recovered $(Ph_4P)_2[Pd_2I_6]$ against six bacterial strains is demonstrated in Figure 9. The organisms evaluated in this study were sensitive towards the compound. Among the bacterial strains, *K. pneumoniae* recorded the highest inhibition zone in all $(Ph_4P)_2[Pd_2I_6]$ concentrations. *B. subtilis*, *S. typhimurium, K. pneumoniae*, and *K. aeruginosa* cultures demonstrated a significant increase in inhibition zone from the lowest to the highest $(Ph_4P)_2[Pd_2I_6]$ concentrations, while *B. cereus* and *E. coli* recorded no notable difference.

The positive control Gentamicin employed in this study exhibited an inhibition range between 21.0-24.8 mm. Previous studies have described palladium nanoparticles as useful antimicrobial agent where more inhibitory toward gram-positive bacteria (*Staphylococcus aureus)* than toward *E. coli* [25]. Palladium (II) complexes were also reported to exhibit remarkable antibacterial activity against *S. aureus* and *E.coli* [20].

Gram-negative bacteria possess lipopolysaccharide (LPS), thin peptidoglycans, and porins proteins with more lipids in their cell walls, which make them less permeable than gram-positive bacteria [26]. Nonetheless, the recovered Pd (II) complexes in this study demonstrated a more significant inhibitory toward gram-negative bacteria. The findings suggested that the complexes could compromise the membrane permeability of the gram-negative bacteria employed. A

significant inhibition improvement in at least one gram-positive bacteria, *B. subtilis*, was also recorded. A previous study supported the current results, in which Pd dichloride ligands ($PdCl_2$BLs) documented the best response against *E. coli, Pseudomonas aeruginosa, S. aureus*, and *B. subtilis* [27].

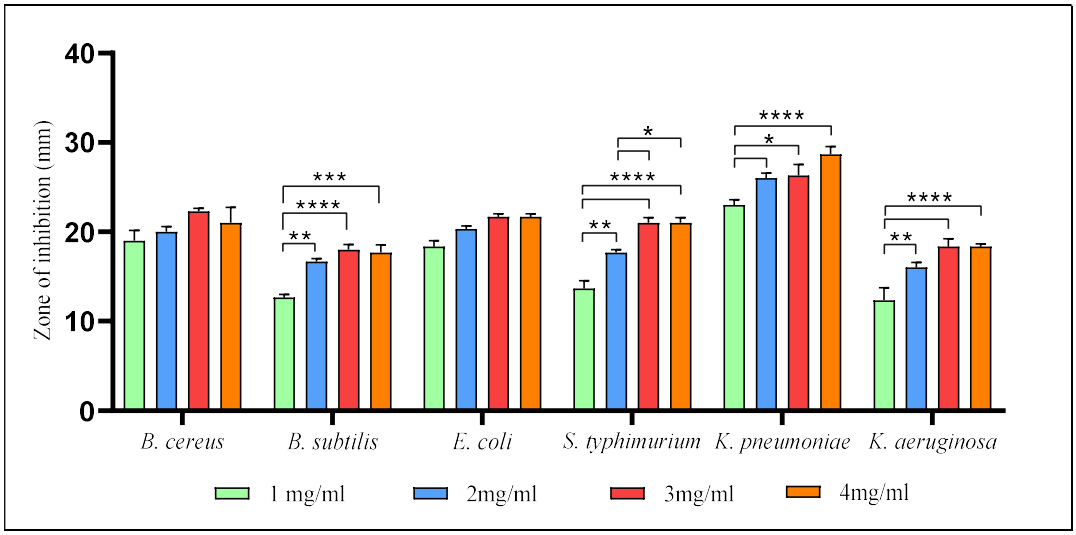


Figure 9. The inhibition zones of the recovered $(Ph_4P)_2[Pd_2I_6]$ against selected bacterial strains. The levels displayed are the mean of three tested cultures ± SEM. The asterisks indicate statistically significant differences analyzed with two-way ANOVA followed by Tukey's multiple comparison post-test

**Determination of MIC and MBC**

Table 3 summarises the MIC values obtained in the present study. Both *Klebsiella* species were inhibited at 0.625 mg/ml, while *E. coli* and *S. typhimurium* were at 0.156 and 0.313 mg/mL, respectively. The recovered $(Ph_4P)_2[Pd_2I_6]$ also hindered *B. cereus* growth at 0.156 mg/mL. The highest MIC value was recorded by *B. subtilis* at 1.25 mg/mL.

The study findings highlighted the potential of the $(Ph_4P)_2[Pd_2I_6]$ procured to inhibit the growth of bacteria. All MBC plates employed in the present study demonstrated bacterial growth, indicating no bactericidal activity when exposed to the $(Ph_4P)_2[Pd_2I_6]$ complex (see Table 4). Nevertheless, uncertainties remain about the killing properties of the recovered $(Ph_4P)_2[Pd_2I_6]$. Accordingly, further studies are necessary to assess the bactericidal potential of $(Ph_4P)_2[Pd_2I_6]$.

## Conclusion

The present study emphasized the utilization of commercially available iodine and tetrabutylammonium iodide to recover Pd metals from TWC waste. The recovered $(Ph_4P)_2[Pd_2I_6]$ complexes were employed directly as a homogeneous catalyst in the C-H functionalization of benzo[*h*]quinoline and 8-methylquinoline. An excellent product yield of 90% was obtained in benzo[*h*]quinoline methoxylation at 100°C. A milder and safer approach adopted at a low-temperature setup (50°C) produced a similar product yield. Conversely, installing the ethoxy- and isopropoxy functional groups into the benzo[*h*]quinoline at 50°C proved challenging. A lower to moderate product yield was recorded due to the solvent stearic effect. Similarly, a reasonable procurement (65%) of 8-(methoxymethyl) quinoline was documented.

In conclusion, the novel method of employing Pd complex as a homogeneous catalyst in C-H functionalization would increase the value of the metal, especially when recovered from TWC waste. Furthermore, the burden on natural reserves as a primary source would also be reduced. This study has also

identified the bacteriostatic potential of the $(Ph_4P)_2[Pd_2I_6]$ complexes. The data provide critical preliminary insights into the role of the metal as an antibacterial agent.

Table 3. The MIC of the recovered $(Ph_4P)_2[Pd_2I_6]$ against selected bacterial strains

| Bacteria | **$(Ph_4P)_2[Pd_2I_6]$ concentration (mg/mL)** | | | | | | | | |
|---|---|---|---|---|---|---|---|---|---|
| | 10 | 5 | 2.5 | 1.25 | 0.625 | 0.313 | 0.156 | 0.078 | Positive control |
| *E. coli* | - | - | - | - | - | - | - | + | + |
| *S. typhimurium* | - | - | - | - | - | - | + | + | + |
| *K. pneumoniae* | - | - | - | - | - | + | + | + | + |
| *K. aeruginosa* | - | - | - | - | - | + | + | + | + |
| *B. cereus* | - | - | - | - | - | - | - | + | + |
| *B. subtilis* | - | - | - | - | + | + | + | + | + |

Table 4. The MBC of the $(Ph_4P)_2[Pd_2I_6]$ against selected bacterial strains

| **Bacteria** | **Minimum bactericidal concentration (mg/ml)** | | | | | | | | |
|---|---|---|---|---|---|---|---|---|---|
| | 10 | 5 | 2.5 | 1.25 | 0.625 | 0.313 | 0.156 | 0.078 | Positive control |
| *E. coli* | + | + | + | + | + | + | + | + | + |
| *B. cereus* | + | + | + | + | + | + | + | + | + |
| *B. subtilis* | + | + | + | + | + | + | + | + | + |
| *S. typhimurium* | + | + | + | + | + | + | + | + | + |
| *K. pneumoniae* | + | + | + | + | + | + | + | + | + |
| *K. aeruginosa* | + | + | + | + | + | + | + | + | + |

Note: (+) denotes bacterial growth and (-) killed bacterial growth

**Acknowledgement**

The authors wish to acknowledge the Ministry of Higher Education Malaysia for providing financial support through the Fundamental Research Grant Scheme (FRGS)-RACER, grant code: 600-IRMI/FRGS-RACER 5/3 (069/2019) and scholarship under the Post-Doctoral Training Scheme, grant code KPT(BS)820710105709. The authors would also like to extend their gratitude to the Faculty of Applied Sciences and Institute of Science, UiTM and Imperial College London for the support and facilities provided.

**References**

1. Wilburn, D. R., and Bleiwas, D. I. (2004). Platinum-group metals—world supply and demand. *US geological survey open-file report*, 1224:2004-1224.
2. McCarthy, S., Braddock, D. C., and Wilton-Ely, J. D. (2021). Strategies for sustainable palladium catalysis. *Coordination Chemistry Reviews*, 442: 213925.
3. Hagelüken, C. (2006). Markets for the catalyst metals platinum, palladium and rhodium. *Metall-Berlin,* 60(1): 31-42.
4. Hagelüken, C., and Umicore, A. G. (2012). Recycling the Platinum Group Metals: A European Perspective, Effective recycling systems for pgm-containing materials will ensure sustainable supply. *Platinum Metals Reviews*, 56(1): 29-35.
5. Sing Singh, P. K., Singh, R. S., and Singh, S. (2016). Environmental and social impacts of mining and their mitigation. In *Kolkata (India): National Seminar ESIMM-2016*.
6. Stocks, J., Blunden, J. R., and Down, C. G. (1974). Metal Mining and the Environment. *American Geological Institute: Alexandria, VA, USA*.
7. Glaister, B. J., and Mudd, G. M. (2010). The environmental costs of platinum–PGM mining and sustainability: Is the glass half-full or half-empty?. *Minerals Engineering*, 23(5):438-450.

8. Yousif, A. M. (2019). Recovery and then individual separation of platinum, palladium, and rhodium from spent car catalytic converters using hydrometallurgical technique followed by successive precipitation methods. *Journal of Chemistry*, 2019: 7.
9. Chen, M., Avarmaa, K., Klemettinen, L., O'Brien, H., Sukhomlinov, D., Shi, J., and Jokilaakso, A. (2020). Recovery of precious metals (Au, Ag, Pt, and Pd) from urban mining through copper smelting. *Metallurgical and Materials Transactions B*, 51(4): 1495-1508.
10. Benson, M., Bennett, C. R., Harry, J. E., Patel, M. K., and Cross, M. (2000). The recovery mechanism of platinum group metals from catalytic converters in spent automotive exhaust systems. *Resources, Conservation and Recycling*, 31(1): 1-7.
11. Hunt, A. J. (Ed.). (2013). *Element recovery and sustainability* (No. 22). Royal Society of Chemistry.
12. Serpe, A., Bigoli, F., Cabras, M. C., Fornasiero, P., Graziani, M., Mercuri, M. L., and Deplano, P. (2005). Pd-dissolution through a mild and effective one-step reaction and its application for Pd-recovery from spent catalytic converters. *Chemical Communications*, 8: 1040-1042.
13. Jantan, K. A., Kwok, C. Y., Chan, K. W., Marchiò, L., White, A. J., Deplano, P., and Wilton-Ely, J. D. (2017). From recovered metal waste to high-performance palladium catalysts. *Green Chemistry*, 19(24): 5846-5853.
14. Dick, A. R., Hull, K. L., and Sanford, M. S. (2004). A highly selective catalytic method for the oxidative functionalization of C− H bonds. *Journal of the American Chemical Society*, 126(8): 2300-2301.
15. Cuscusa, M., Rigoldi, A., Artizzu, F., Cammi, R., Fornasiero, P., Deplano, P., and Serpe, A. (2017). Ionic couple-driven palladium leaching by organic triiodide solutions. *ACS Sustainable Chemistry & Engineering*, 5(5): 4359-4370.
16. Arafath, M. A., Adam, F., and Hassan, M. Z. (2021). Synthesis, characterization, X-ray crystal structure and antibacterial activity of nickel, palladium and platinum complexes with Schiff base derived from N-cyclohexylhydrazinecarbothioamide and 5-(tert-butyl)-2-hydroxybenzaldehyde. *Phosphorus, Sulfur, and Silicon and the Related Elements*, 196(6): 530-537.
17. Mallikarjuna, K., Nasif, O., Ali Alharbi, S., Chinni, S. V., Reddy, L. V., Reddy, M. R. V., and Sreeramanan, S. (2021). Phytogenic synthesis of Pd-Ag/rGO nanostructures using stevia leaf extract for photocatalytic H2 production and antibacterial studies. *Biomolecules*, 11(2): 190.
18. Anju, A. R. Y. A., Gupta, K., and Chundawat, T. S. (2020). In vitro antimicrobial and antioxidant activity of biogenically synthesized palladium and platinum nanoparticles using Botryococcus braunii. *Turkish Journal of Pharmaceutical Sciences*, 17(3): 299.
19. Chlumsky, O., Purkrtova, S., Michova, H., Sykorova, H., Slepicka, P., Fajstavr, D., and Demnerova, K. (2021). Antimicrobial properties of palladium and platinum nanoparticles: A new tool for combating food-borne pathogens. *International Journal of Molecular Sciences*, 22(15): 7892.
20. Rîmbu, C., Danac, R., and Pui, A. (2014). Antibacterial activity of Pd (II) complexes with salicylaldehyde-amino acids Schiff bases ligands. *Chemical and Pharmaceutical Bulletin*, 62(1): 12-15.
21. Bandyopadhyay, N., Das, M., Samanta, A., Zhu, M., Lu, L., and Naskar, J. P. (2017). Promising antimicrobial activity of an oxime based palladium (II) complex. *ChemistrySelect*, 2(1): 230-240.
22. Haddad, B., Paolone, A., Villemin, D., Taqiyeddine, M., Belarbi, E. H., Bresson, S., and Kiefer, J. (2017). Synthesis, conductivity, and vibrational spectroscopy of tetraphenylphosphonium bis (trifluoromethanesulfonyl) imide. *Journal of Molecular Structure*, 1146:203-212.
23. Kubota, M., Ohba, S., and Saito, Y. (1991). Structure of trans-diiodobis (triphenylphosphine) palladium (II)–trichloromethane (1/1). *Acta Crystallographica Section C: Crystal Structure Communications*, 47(8): 1727-1729.
24. Dumas, A., and Couvreur, P. (2015). Palladium: a future key player in the nanomedical field?. *Chemical Science*, 6(4): 2153-2157.

25. Adams, C. P., Walker, K. A., Obare, S. O., and Docherty, K. M. (2014). Size-dependent antimicrobial effects of novel palladium nanoparticles. *PloS One*, 9(1): e85981.
26. Silhavy, T. J., Kahne, D., and Walker, S. (2010). The bacterial cell envelope. *Cold Spring Harbor Perspectives in Biology*, 2(5): a000414.
27. Sharma, N. K., Ameta, R. K., and Singh, M. (2016). From synthesis to biological impact of Pd(II) complexes: synthesis, characterization, and antimicrobial and scavenging activity. *Biochemistry Research International*, 2016: 4359375.